

An analysis of energy expenditure in Goodwin Creek

Peter Molnár and Jorge A. Ramírez

Department of Civil Engineering, Colorado State University, Fort Collins

Abstract. The local optimality hypothesis that natural river systems adjust their average channel properties toward an optimal state in which the rate of energy dissipation per unit channel area, P_a , is constant throughout the river network is explored on an analysis of Goodwin Creek, Mississippi. River network parameters describing the variation of channel forming and maintaining discharge, channel downstream hydraulic geometry, bed slope, and sediment concentration as a function of cumulative drainage area are estimated from Goodwin Creek data. Optimal channel characteristics that produce constant P_a are determined and superposed onto the digital elevation model–extracted river network with reach averaged bed slopes, and the spatial distribution of the energy dissipation rate P_a throughout the network is analyzed. Channel reaches with average energy dissipation rates different from the constant value of the optimal network are identified. We argue that these reaches are potentially unstable relative to the remainder of the network, and that their average channel properties will adjust in the direction of constant P_a . Qualitative statements are made about the direction of this adjustment through differences between the observed and optimal channel widths, and comparisons are made with recent observations of channel change in Goodwin Creek. This energy expenditure analysis suggests that the hypothesis of local optimality can be a useful tool for studying the relative stability and potential channel adjustment of river networks.

1. Introduction

The topological structure of a river network and the distribution of its channel characteristics reflect the conditions of the watershed through a complex interaction of channel properties, basin topography, hydrologic conditions, and sediment transport. Researchers have attempted to define an equilibrium state where the external driving conditions, watershed properties, and river network are in balance using concepts of energy expenditure. Since a river network constantly performs work and dissipates energy by transporting water and sediment, it has been theorized that drainage networks develop into optimal states in which least energy is spent [Leopold and Langbein, 1962; Langbein, 1964; Langbein and Leopold, 1964]. Theories of minimum stream power and energy dissipation rate have been developed to describe channels in equilibrium with their water and sediment discharge [Yang 1971; Yang and Song, 1979, 1986], and utilized in describing the topological structure and shape of river networks [Howard, 1990; Rodríguez-Iturbe *et al.*, 1992a]. Rodríguez-Iturbe *et al.* [1992a] postulated three principles of optimality in energy expenditure that related the three-dimensional structure of the river network and its individual elements to the rate of energy expenditure. Combining these three principles led to the definition and modeling of optimal channel networks (OCNs) [e.g., Rinaldo *et al.*, 1992; Rigon *et al.*, 1993].

The principles of Rodríguez-Iturbe *et al.* [1992a] are restated in this paper in two hypotheses of optimality in energy expenditure: (1) The local optimal energy expenditure hypothesis states that river networks will adjust their channel properties toward an optimal state in which the energy dissipation rate per unit channel area P_a throughout the network is constant.

(2) The global optimal energy expenditure hypothesis states that river networks will adjust their topological structure toward an optimal state in which the total energy dissipation rate P_t in the network is minimum. River systems constantly respond to spatially and temporally variable external driving forces of discharge and sediment load by adjusting their shape and form. At the same time, they develop average conditions (such as average downstream hydraulic geometry) that are relatively stable on an appropriate timescale [Leopold and Maddock, 1953; Knighton, 1984, p. 162]. We argue that this long-term average behavior is a result of efficiency in energy expenditure as expressed by the hypothesis of local optimality. Molnár and Ramírez [this issue] have shown that the local optimality hypothesis can be utilized to determine optimal channel characteristics for a river network in which the energy dissipation rate P_a is constant, and that these optimal channel characteristics are remarkably similar to those of many natural river systems in their downstream hydraulic geometry exponents, distribution of average flow velocity, boundary shear, resistance to flow, etc. However, natural river networks continuously adjust, and fluctuations will occur in time and space around the optimal state depending on external driving conditions of streamflow and sediment supply, geologic and other constraints, and the response of the network to those conditions [Petts and Foster, 1985]. We theorize that in a river network, deviations of average behavior from the local optimality condition of constant P_a are a measure of the network's potential instability and adjustment. To show the potential of the hypothesis of local optimality in describing network stability and channel adjustment, we conducted an analysis of energy expenditure in Goodwin Creek, Mississippi.

The expression for the rate of energy dissipation per unit channel area P_a used throughout this study is analyzed in section 2. Using scaling relationships between channel characteristics and drainage area estimated for Goodwin Creek in

Copyright 1998 by the American Geophysical Union.

Paper number 98WR00982.
0043-0397/98/98WR-00982\$09.00

section 3, we determine optimal channel characteristics for the river network in section 4. We then use these optimal channel characteristics together with the digital elevation model (DEM)–extracted topography of Goodwin Creek (thereby allowing channel bed slopes to vary in space), to obtain the distribution of P_a in the river network in section 5. Finally, we study the deviation of this distribution from the constant value of P_a of the optimal network, and identify reaches associated with the deviation. If the local optimality hypothesis is valid, then these reaches will tend to compensate for the departure from local optimality by adjusting their average channel properties from the predicted optimal values in the direction of constant P_a . We investigate this thesis on the distribution of channel top width in Goodwin Creek in section 6. Our results are compared with available observations of the channel network.

2. Rate of Energy Dissipation per Unit Channel Area

As potential energy of water on the hillslopes is transformed into kinetic energy of the flowing fluid-sediment mixture in the runoff process, energy is dissipated from the system [e.g., *Yang and Song*, 1986]. In our analysis, the rate of energy dissipation defines the work that a fluid element needs to perform to overcome friction at the boundary. Dividing the river network into a series of links with rectangular cross-sections and assuming (1) one-dimensional uniform flow, (2) approximate equality of tangential shear stresses and velocity gradients at the bed and banks in the downstream direction, and (3) fluid incompressibility, and neglecting the effects of linear deformation of a particle by tension against the banks or water surface, gives the rate of energy dissipation in a link P_i [e.g., *Molnár and Ramírez*, this issue]:

$$P_i = LP_w\tau_0\nu = \gamma_mLSQ \quad (1)$$

where L is the channel link length, P_w is its wetted perimeter, τ_0 is an average boundary shear stress, S is channel bed slope, Q is discharge and γ_m is the submerged specific weight of the fluid-sediment mixture. In (1) it is also assumed that most energy dissipation occurs in a boundary layer in which shear stress remains constant and the actual velocity is equal to the depth-averaged velocity v . The effect of sediment load on energy dissipation in (1) is in the form of added weight to the fluid-sediment mixture in γ_m .

The energy dissipation rate per unit channel area P_a throughout the network can then be computed as $P_a = P_i/P_wL$ and, using (1), becomes

$$P_a = g\rho_w[1 + C_{Vp}(G - 1)]S \frac{Q_p}{W_p + 2H_p} \quad (2)$$

where $\gamma_m = g\rho_w[1 + C_{Vp}(G - 1)]$, g is gravitational acceleration, ρ_w is the density of water, G is the specific gravity of sediment, and C_{Vp} is the total volumetric sediment concentration. The subscript p represents the discharge frequency (exceedance probability), and W_p and H_p are the channel flow width and depth corresponding to discharge Q_p . The crucial problem in determining the energy dissipation rate P_a throughout a river network lies in identifying the discharge, corresponding channel cross-sectional geometry, slope, and sediment concentration characteristics in (2) throughout the network. These variables can be related to the area draining to the channel network. Drainage area is a quantity that is easily

defined from DEMs as the cumulative number of pixels draining to each pixel belonging to the extracted network.

Molnár and Ramírez [this issue] use the following expressions to relate discharge, channel, and sediment characteristics in (2) to drainage area A :

$$Q_p = \psi_p A^{\theta(p)} \quad (3a)$$

$$H_p = c_p Q_p^f = c_p \psi_p^f A^{f\theta(p)} \quad (3b)$$

$$W_p = a_p Q_p^b = a_p \psi_p^b A^{b\theta(p)} \quad (3c)$$

$$C_{Vp} = k_p Q_p^j = k_p \psi_p^j A^{j\theta(p)} \quad (3d)$$

$$S = sA^z \quad (3e)$$

River network parameters are the scaling coefficients of relations (3a) to (3e), which need to be estimated from watershed data. Discharge scaling parameters are ψ_p and $\theta(p)$. Channel geometry is described by the downstream hydraulic geometry relations of *Leopold and Maddock* [1953] with the scaling parameters for flow depth c_p , f , and flow width a_p , b . Total sediment concentration parameters are k_p and j . Channel bed slope scaling parameters are s and z .

The energy dissipation rate P_a throughout a river network then becomes [*Molnár and Ramírez*, this issue]

$$P_a = g\rho_w \frac{s\psi_p A^{\theta(p)+z} + (G - 1)k_p s \psi_p^{j+1} A^{(j+1)\theta(p)+z}}{a_p \psi_p^b A^{b\theta(p)} + 2c_p \psi_p^f A^{f\theta(p)}} \quad (4)$$

Relating river network variables independently to drainage area is possible only in the context of their long-term average behavior [*Troutman*, 1996; *Molnár and Ramírez*, this issue]. The expression for P_a in (4) then describes the distribution of energy expenditure under such conditions.

3. Goodwin Creek Watershed Data Analysis

Goodwin Creek is an experimental watershed situated in Panola County, Mississippi, administered by the National Sedimentation Laboratory of the U.S. Department of Agriculture's Agricultural Research Service in Oxford. Its purpose is to provide data for the estimation of impacts of upstream land use and watershed processes on sediment supply, sediment transport in streams, and channel stability. The watershed is well instrumented to measure streamflow, sediment load, precipitation, channel characteristics, soil and land use characteristics, and other watershed parameters and was chosen for the analysis of energy expenditure in this study because of this data abundance. This section presents general information about the Goodwin Creek river network and the estimation of river network parameters.

3.1. General Description

The Goodwin Creek watershed is located in the bluff hills region of north central Mississippi. The watershed area is approximately 21.4 km², with elevation ranging between 66 and 129 meters above sea level. Goodwin Creek is a tributary of Long Creek, which flows into the Yocona River (one of the main rivers of the Yazoo River Basin). We extracted the Goodwin Creek river network from a 30 × 30 m DEM by determining flow directions using the steepest slope D8 method [e.g., *Tarboton*, 1997] and computing contributing area to each cell. A constant drainage area threshold A_t was used to determine the beginning of the active fluvial section of the

network. Figure 1 shows the extracted network, with $A_t = 0.18 \text{ km}^2$, that we used in this study. The DEM-extracted network compares well with streams depicted on topographic maps of the area. The watershed is divided into 14 subbasins with a flow-measuring flume and gaging station constructed at each subbasin outlet (Figure 1). Continuous measurements of streamflow and sediment load are made at these gaging stations [Blackmarr, 1995].

The Goodwin Creek watershed is largely free of land management activities, with only 13% of its total area being cultivated [Kuhnle *et al.*, 1996]. The climate is humid, with hot summers and mild winters. Average annual precipitation is 1400 mm y^{-1} , and the average annual air temperature is about 17°C . Major runoff events associated with intense erosion are commonly a result of severe thunderstorms in late winter or spring. The terrain of the watershed consists of broad ridges and relatively narrow valleys filled with alluvial deposits [Blackmarr, 1995]. The predominant soil material is silty in texture and is easily eroded when the vegetative cover is removed. Historically, erosion has been a problem at Goodwin Creek. Particularly severe erosion was initiated by deforestation and intensive cotton agriculture in the 1830s and led to channelization of some sections of the network in order to prevent further degradation. Incision is still in progress in many streams, producing widespread problems of bank stability [Grissinger and Murphey, 1986, 1989; Kuhnle *et al.*, 1996].

We first conducted a quantitative analysis of the structure of Goodwin Creek DEM-extracted river networks. For river networks extracted with the threshold area A_t between 0.045 km^2 and 0.18 km^2 , the highest stream order was 4. A study of Horton's laws of stream numbers and lengths for these networks gave an average bifurcation ratio $R_B = 3.55$ and an average stream length ratio $R_L = 2.83$ [Molnár, 1996]. This is consistent with results from most natural river systems, where the value of R_B has been found to vary in the range between 2 and 4 and R_L has been found to vary between 1.5 and 3.5 [e.g., Bras, 1990]. We also studied the cumulative distribution of area draining to the river network. Rodríguez-Iturbe *et al.* [1992b] found this distribution to follow a power law of the form $P[A \geq a] \propto a^{-\beta}$, with $\beta \approx 0.45$ consistent among many basins. The distribution of cumulative drainage area for the Goodwin Creek extracted network with $A_t = 0.18 \text{ km}^2$ is shown in Figure 2. The probability of exceeding the threshold

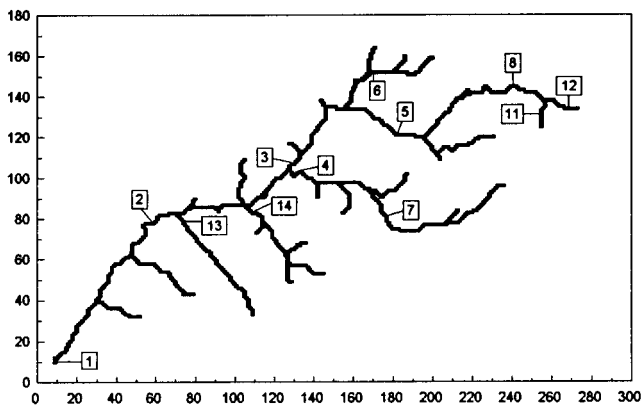


Figure 1. Goodwin Creek river network extracted from a $30 \times 30 \text{ m}$ DEM with threshold area $A_t = 0.18 \text{ km}^2$ (200 cells), together with the location of gaging stations used in the energy expenditure analysis (1 unit = 30 m).

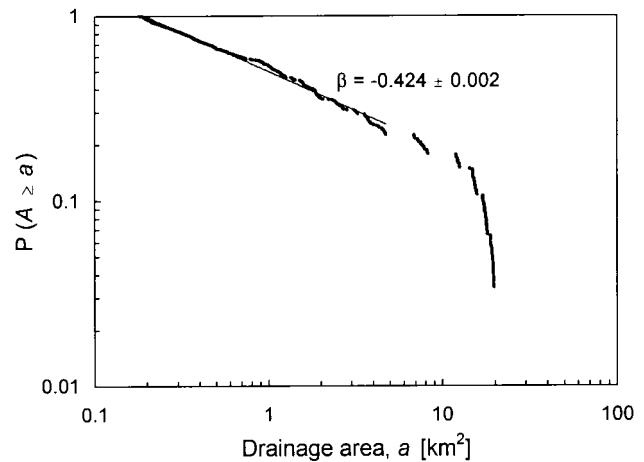


Figure 2. Cumulative distribution of drainage area in the Goodwin Creek network.

area A_t that defines a channel is equal to 1 in the river network. From this point, the distribution of drainage areas decreases in a well-defined power law form with $\beta = 0.424 \pm 0.002$ up to a drainage area of 4.7 km^2 . The value of the exponent β is very similar to the results of other researchers [e.g., Rinaldo *et al.*, 1992; Rigon *et al.*, 1993]. Since the basin is small, the power law relationship persists only over one log scale. It then breaks down at large drainage areas owing to a finite size effect [Rodríguez-Iturbe and Rinaldo, 1997, p. 135]. The average drainage area of the Goodwin Creek DEM-extracted river network with $A_t = 0.18 \text{ km}^2$ is 4.29 km^2 .

3.2. Estimation of River Network Parameters

3.2.1. Discharge. River network parameters for driving discharge conditions that need to be estimated from data are the scaling constant ψ_p and the scaling exponent $\theta(p)$ in (3a). Instantaneous stage measurements are available at each of the 14 gaging stations in the Goodwin Creek watershed [Bowie and Sansom, 1986; Blackmarr, 1995]. The flow regime at Goodwin Creek is flashy, and over 77% of the annual runoff amount comes during the wet period between December and May. The observed maximum flow at the watershed outlet was in February at $32.2 \text{ m}^3 \text{ s}^{-1}$. Minimum flows at that station fluctuate between 4.2 and $10.5 \times 10^{-3} \text{ m}^3 \text{ s}^{-1}$, indicating almost dry channel conditions [Blackmarr, 1995]. Drainage areas above each gaging station range from 0.06 km^2 to 21.41 km^2 at the outlet. Upstream sections of the Goodwin Creek river network are ephemeral in nature [Kuhnle, 1992; Blackmarr, 1995]. Because of this, we used the drainage area threshold $A_t = 0.18 \text{ km}^2$ to define the active river network with mostly continuous streamflow records, and we omitted two gaging stations (9 and 10) draining an area less than A_t from further analyses. The locations of the 12 gaging stations used hereafter are shown in Figure 1.

The conversion from stage measurements to discharge for each gaging station was computed from discharge rating curves of the form

$$Q = dr_e H^{dr_e} \quad (5)$$

where dr_e is the discharge rating curve constant and dr_e is the discharge rating curve exponent. These rating curve parameters depend on the structural characteristics of the flumes. For the purpose of this study, we computed average rating curve

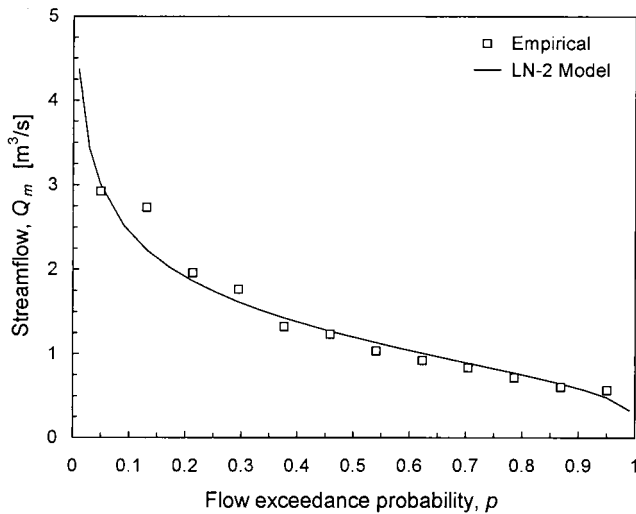


Figure 3. Empirical and fitted LN-2 model flow duration curves for maximum monthly streamflows at station 1 on Goodwin Creek.

parameters for the whole range of flows observed at each station from available data [Molnár, 1996].

The energy expenditure analysis is based on the presumption that discharge is of sufficient magnitude to control channel geometry. Because of the flashy nature of streamflow at Goodwin Creek, the determination of dominant characteristic discharge in the energy expenditure framework is not simple. In this study we investigated two characteristic discharge conditions: maximum monthly streamflow condition and maximum daily streamflow condition. Maximum monthly flow in any given water year represents longer-term driving conditions for the response of the river network and can be viewed as the channel-maintaining discharge. Maximum daily flow in any given water year represents higher-magnitude flows with low frequency of occurrence that induce rapid channel changes, and can be viewed as the channel-forming discharge.

We conducted analyses of the frequency and spatial distri-

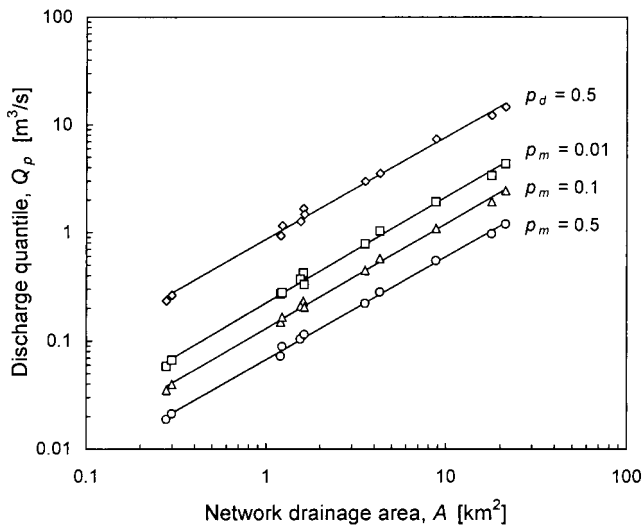


Figure 4. Scaling analysis of maximum monthly and daily discharge quantiles (with exceedance probability p) as a function of cumulative drainage area.

bution of maximum monthly and daily streamflow. The data period used in the frequency analysis was equal at all stations, and covered 12 water years between 1982 and 1993. Because of the short records and the fact that the computed skewness coefficient for maximum monthly data was greater than 1.0 for most stations, the two-parameter lognormal (LN-2) probability distribution model was used to fit the streamflow data using the method of moments at all studied stations. From the LN-2 model, discharge quantiles Q_p with exceedance probabilities $p_m = 0.5$, $p_m = 0.1$, and $p_m = 0.01$ for maximum monthly data were determined. Discharge quantiles for maximum daily streamflow with exceedance probability $p_d = 0.5$ were determined from the empirical probability density function. An example of the flow duration curve for maximum monthly streamflow at station 1 constructed using the LN-2 model is shown in Figure 3 and compared with the empirical flow duration curve [Molnár, 1996]. The empirical values were plotted from data using the plotting position $p_i = 1 - (i - 0.4)/(n + 0.2)$ recommended for obtaining nearly quantile-unbiased plotting positions for a range of distributions [Stedinger et al., 1992], where i represents the order of the streamflow value in a descending series of n values. The quantiles Q_p were then related to drainage area at the 12 stations in the form of (3a). Figure 4 shows the plot of Q_p versus A , and the resulting best fit parameters ψ_p and $\theta(p)$ are in Table 1. The scaling exponent $\theta(p)$ is practically independent of p , indicating simple scaling [e.g., Gupta et al., 1994; Gupta and Dawdy, 1995]. The value of the scaling exponent close to 1 suggests that the entire drainage area is employed in runoff production at the studied streamflow conditions.

3.2.2. Channel hydraulic geometry. The systematic variation in channel cross-sectional geometry throughout a river network is described in this study by the downstream hydraulic geometry relations of Leopold and Maddock [1953]. They relate the average flow depth and width to discharge of the same frequency throughout the network. River network parameters that describe the variation of channel flow depth downstream are the scaling constant c_p and the hydraulic geometry exponent f in (3b). In order to be able to estimate the scaling parameters c_p and f , we made the assumption that flow depths at the gaging station flumes are approximately equal to the flow depths in the channel reaches at those locations. Using the rating curves in (5), we then computed the flow depths corresponding to discharges of studied frequencies at each gaging station and estimated the parameters c_p and f . The results are in Table 2. It was not possible to calibrate the relation (3c) for channel flow width, because the width measurements of channels from surveys throughout Goodwin Creek are not related to a particular discharge magnitude or frequency. However, the downstream variation of channel flow width was computed by applying the local optimal energy expenditure hypothesis to

Table 1. Discharge Scaling Parameters of the Relation $Q_p = \psi_p A^{\theta(p)}$

p	ψ_p	$\theta(p)$	R^2
$p_m = 0.5$	0.0675	$0.949 \pm 0.019^*$	0.998
$p_m = 0.1$	0.1310	0.966 ± 0.021	0.998
$p_m = 0.01$	0.2247	0.979 ± 0.026	0.996
$p_d = 0.5$	0.8684	0.950 ± 0.030	0.995

Here Q is in cubic meters per second, and A is in square kilometers. *90% confidence limits.

Goodwin Creek, as will be seen later. In the process of river adjustment, channel geometry is commonly thought to be the first to change, and it therefore plays an important role in the energy expenditure framework [e.g., *Knighton*, 1984, p. 162].

3.2.3. Sediment concentration. River network parameters that describe the downstream variation of the volumetric sediment concentration are the scaling constant k_p and exponent j in (3d). Continuous measurements of fine sediment in suspension (particle diameter less than 0.062 mm) are made by point automated pumping sediment samplers at each of the flumes located at Goodwin Creek gaging stations [Bowie and Sansom, 1986; Willis et al., 1986; Blackmarr, 1995]. The samplers also measure a fraction of the transport of sand (particle diameter 0.062 mm to 2 mm). However, these measurements are not very reliable, mainly because the transport rate of sand-sized sediment varies within the cross section. In addition, systematic manual sampling of sand and gravel-sized sediment in transport by depth-integrated suspended sediment samplers and bed load samplers is conducted [Blackmarr, 1995; Kuhnle, 1996].

We constructed monthly suspended sediment rating curves for all analyzed gaging stations from data that relate average monthly suspended sediment load Q_s in kilograms per second to average monthly discharge Q in cubic meters per second:

$$Q_s = sr_c Q^{sr_e} \quad (6)$$

where sr_c and sr_e are the sediment rating curve constant and exponent, respectively. The monthly suspended sediment rating curve for station 1 is shown in Figure 5 (constructed from the period 1982–1993) [Molnár, 1996]. The problem remained to estimate the total rate of sediment transport. *Kuhnle et al.* [1989] identified the fractions of fines, sand, and gravel in the total sediment yield from Goodwin Creek measured at station 2. Their results show that in the period 1984–1988, fines and sand were the dominant sediment sizes. On the average, 59% of the transported sediment was in the fine material range, and 39% was sand. This means that the suspended sediment rating curves developed above would account for over two thirds of the total sediment load. *Kuhnle et al.* [1996] showed that gravel bed load accounts for only about 5% of total sediment load, as flows in the channels sufficient to move the coarsest bed sediment occur on average only 12 times a year.

To account for sand and gravel in transport, we multiplied the suspended sediment concentration by the parameter α to obtain the total concentration of sediment in transport. An estimate of the volumetric concentration C_V of total sediment load can then be obtained as

$$C_V = \alpha \frac{Q_s}{Q_s + \rho_s Q} \quad (7)$$

Table 2. Parameters of the Downstream Hydraulic Geometry Relation for Channel Flow Depth $H_p = c_p Q_p^f$

p	c_p	f	R^2
$p_m = 0.5$	0.3280	$0.317 \pm 0.036^*$	0.937
$p_m = 0.1$	0.3550	0.321 ± 0.036	0.938
$p_m = 0.01$	0.3772	0.324 ± 0.036	0.939
$p_d = 0.5$	0.4337	0.320 ± 0.036	0.938

Here Q_p is in cubic meters per second, and H_p is in meters.
*90% confidence limits.

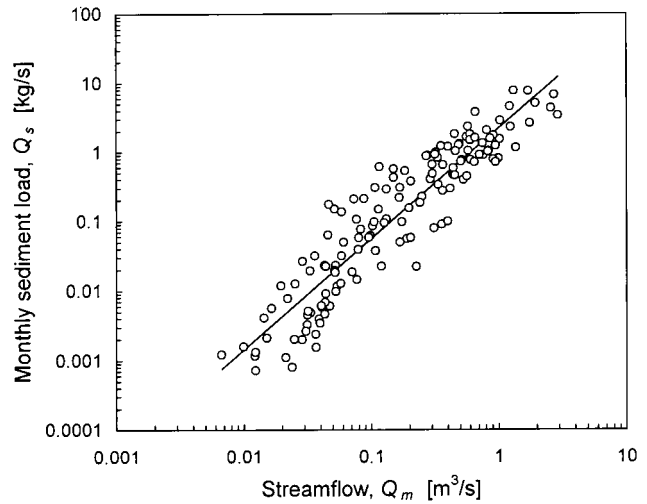


Figure 5. Average monthly suspended sediment rating curve at station 1 on Goodwin Creek.

where ρ_s is the density of sediment. Based on the above analyses of fractional rates of sediment transport at Goodwin Creek and our studied discharge conditions, an estimate of $\alpha = 2$ was chosen in this study.

We analyzed the spatial distribution of sediment concentration by relating C_V to discharge of studied frequencies at every gaging station as in (3d) for maximum monthly streamflows only, where total sediment concentrations were calculated using equations (6) and (7). The resulting scaling constants k_p and scaling exponents j are given in Table 3. Total concentrations increase downstream, and the computed maximum total sediment concentration at the outlet of Goodwin Creek was approximately $C_V = 0.003$ (7900 ppm). For the maximum daily streamflow condition a constant sediment concentration $C_V = 0.003$ was used.

3.2.4. Channel bed slope. The analysis of channel bed slopes in the Goodwin Creek network was conducted on the DEM of the basin. We divided the river network into 17 reaches, depicted in Figure 6, and computed the elevation drop ΔH between the top and bottom of each reach as well as the length L along the channel of the reach. Assuming that channel reach slopes approximately follow the surface slopes of the terrain, the average channel slope S in each reach was computed as $S = \Delta H/L$. The computed slopes of reaches 11, 13, and 17 on the main stem were about 0.001, while for the remainder of the network computed slopes ranged from about 0.003 to 0.022. The reach slopes obtained in this way are slightly higher than the channel survey slopes reported by

Table 3. Parameters of the Total Volumetric Sediment Concentration Scaling Relationship $C_{Vp} = k_p Q_p^j$

p	k_p	j	R^2
$p_m = 0.5$	1.401×10^{-3}	$0.249 \pm 0.099^*$	0.542
$p_m = 0.1$	1.507×10^{-3}	0.339 ± 0.108	0.650
$p_m = 0.01$	1.457×10^{-3}	0.409 ± 0.121	0.685

Here Q_p is in cubic meters per second and C_{Vp} is in cubic meters per cubic meter.

*90% confidence limits.

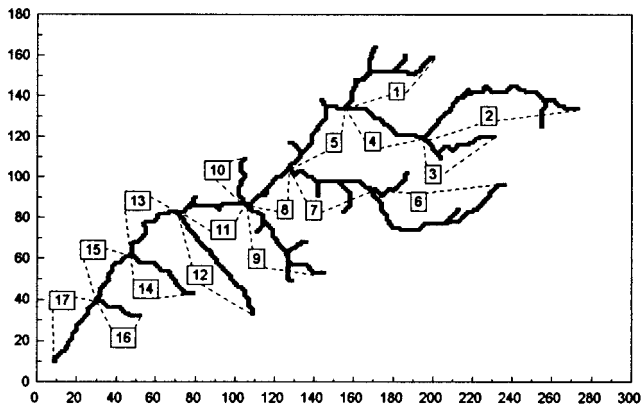


Figure 6. Location of 17 channel reaches on the Goodwin Creek river network.

Blackmarr [1995], especially in the upstream sections of the network.

To estimate the scaling parameters s and z in (3e), we plotted channel reach slope versus average contributing area to each of the 17 Goodwin Creek reaches in Figure 7. The river network in our study was defined as the active fluvial section draining areas larger than 0.18 km^2 . As a result, the different scaling regimes between slope and contributing area observed in the hillslope, unchanneled valley, and channeled valley sections were not of concern. *Ijjász-Vásquez and Bras* [1995] report that the change in scaling between unchanneled and channeled portions of the watershed occurs between approximately 0.01 km^2 and 0.1 km^2 .

Two different topographic conditions were explored. The first condition was represented by a constrained slope scaling exponent $z = -0.5$. This is the average value found by *Tarboton et al.* [1989] and others from studies of numerous DEM-extracted networks, and it is also the exponent inherent in the definition of OCNs. For the constrained condition, linear regression on log-transformed data gave $z = -0.5$, $s = 0.0094$ (with a 90% confidence interval 0.0074 – 0.0119), and the determination coefficient $R^2 = 0.664$. The second condition was one in which the scaling exponent z was not constrained. In this

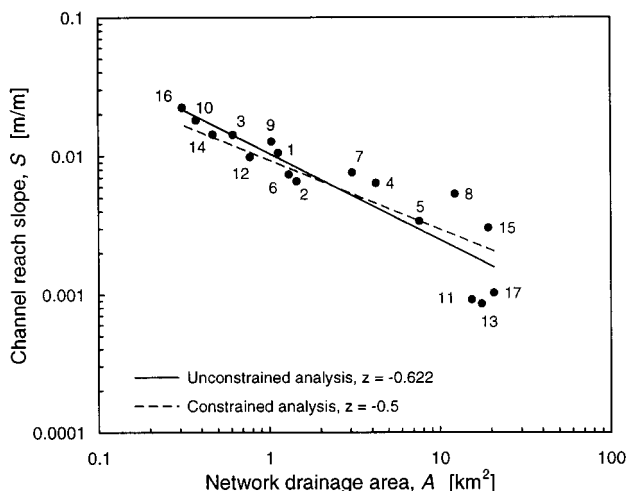


Figure 7. Channel bed slope scaling analysis (unconstrained and constrained topographic conditions) on Goodwin Creek.

case the best fit to Goodwin Creek slope data gave $z = -0.622 \pm 0.037$ (90% confidence limits), $s = 0.0105$ (with a 90% confidence interval 0.0088 – 0.0124), and the determination coefficient $R^2 = 0.826$. Both cases are shown in Figure 7. In the context of our study, the constrained condition represents a river network with higher variability in channel bed slopes around the slope scaling relation in (3e).

4. Optimal Channel Characteristics

The local optimal energy expenditure hypothesis states that in an optimal river network the rate of energy dissipation per unit channel area, P_a , is constant throughout the network. Optimal channel characteristics are the channel characteristics of such a network. In this section we discuss the development of optimal channel characteristics for Goodwin Creek conducted by *Molnár and Ramírez* [this issue] using river network parameters from section 3. Specifically, the downstream variation of channel flow width represented by the exponent b in the downstream hydraulic geometry relation of *Leopold and Maddock* [1953] in (3c) that ensures constant P_a is found.

Since P_a in (4) is a function of drainage area, local optimality will require $d(P_a)/dA = 0$ throughout the network. The derivative will approach zero as a function of river network parameters (b, f, \dots) in (3a)–(3e). In order to find this optimal solution *Molnár and Ramírez* [this issue] defined an optimality function $h(b, f, \dots)$ that finds the optimal set of river network parameters (b^*, f^*, \dots) as

$$h(b^*, f^*, \dots) = \min_{\forall(b, f, \dots)} h(b, f, \dots) \\ = \min_{\forall(b, f, \dots)} \frac{1}{A_0} \int_{A_i}^{A_o} \left| \frac{d[P_a(A; b, f, \dots)]}{dA} \right| A dA \quad (8)$$

In (8), A_i is the drainage area associated with the channel initiation threshold, and A_o is the drainage area at the outlet of the basin. The optimality function h gives more importance to the downstream (mature) sections of a river network by weighing $d(P_a)/dA$ with drainage area.

Using the minimization procedure described above, *Molnár and Ramírez* [this issue] computed the optimal channel flow width variation downstream at Goodwin Creek in the form of (3c) for the studied streamflow and topographic conditions. The optimal downstream hydraulic geometry parameters (a_p and b) that ensured constant P_a throughout the network are listed in Table 4. In order to ensure that the results from different streamflow conditions were comparable, it was necessary to maintain the same channel flow width at the outlet of the basin. Therefore when searching for the optimal width exponent b , *Molnár and Ramírez* [this issue] also continuously

Table 4. Optimal Downstream Hydraulic Geometry Parameters for Channel Flow Width: a_p and b

	$z = -0.5$		$z = -0.622$	
	b opt	a_p opt	b opt	a_p opt
$P_m = 0.5$	0.488	7.560	0.347	8.244
$P_m = 0.1$	0.498	7.182	0.360	8.639
$P_m = 0.01$	0.506	6.820	0.369	8.869
$P_d = 0.5$	0.488	6.516	0.347	10.182

adjusted the coefficient a_p so that channel flow width at the watershed outlet corresponding to the discharge driving conditions remained constant. These required widths at station 1 were computed using relations from *Julien and Wardalam* [1995] (considering that bed material in reach 17 has $d_{50} = 0.97$ mm and the channel bed slope is $S = 0.00203$ for $z = -0.5$ and $S = 0.00156$ for $z = -0.622$), and were adjusted downward by 10% because the flow conditions were less than bankfull in our case. The optimal exponent b is dependent mostly on the topography of the basin expressed by the slope scaling exponent z [Molnár and Ramírez, this issue]. Optimal b varied between 0.488 and 0.506 for $z = -0.5$ and between 0.347 and 0.369 for $z = -0.622$ (depending on the streamflow condition). These optimal values for Goodwin Creek are within the ranges of observations from many natural river systems reported by *Park* [1977] and others.

Molnár and Ramírez [this issue] also compared the developed optimal channel characteristics with available Goodwin Creek data. Average boundary shear stress in the optimal network was found to be higher in the upstream sections but remained fairly constant once drainage areas exceeded about 6 km². Bed shear is indicative of bed load sediment transport. *Kuhnle* [1992] reported bed shear stresses at station 2 on Goodwin Creek during an extensive study of bed load sediment transport. He observed that downstream bed shear stress exceeding about 10 Pa was sufficient to induce bed load sediment transport and that a consistent relationship between bed shear stress and bed load transport rate can be observed for shear stress up to about 35 Pa. The boundary shear stress at station 2 in the Goodwin Creek optimal networks ranged between approximately 5 Pa and 20 Pa (depending on flow condition), and it would be sufficient to induce bed load sediment transport at higher flow conditions. Resistance to flow measured by the Darcy-Weisbach friction factor ff decreased downstream in the optimal network. Channel sections draining less than approximately 2.5 km² had ff in excess of 1.0 (for maximum monthly flows). According to *Bathurst* [1993], this value would correspond to fairly steep (S up to 0.005) and rough (d_{50} up to 100 mm) gravel bed channels. The values of ff for drainage areas above 2.5 km² decreased from ~ 1.0 to 0.4 at the outlet of the basin. According to *Bathurst* [1993], this value would correspond to sand and gravel bed channels with moderate slopes, which qualitatively satisfies the description of the downstream sections of Goodwin Creek [e.g., *Blackmarr*, 1995].

The computed values of discharge, channel bed slope, flow depth, width and velocity, Darcy-Weisbach friction factor, total sediment concentration, constant energy dissipation rate per unit channel area, and boundary shear stress at the outlet of the Goodwin Creek optimal networks for all studied conditions are summarized in Table 5. Total computed volumetric sediment concentrations at station 1 of the optimal networks varied between 0.00148 and 0.0027 (about 3900 ppm and 7100 ppm) for maximum monthly streamflow conditions. Because in this study $\alpha = 2$ in equation (7), the corresponding suspended sediment concentrations at station 1 in the optimal network varied between 1950 ppm and 3550 ppm. *Kuhnle et al.* [1996] reported average observed fine sediment concentrations for 4-month periods at station 1 to be on average between 1000 ppm and 3000 ppm, which corresponds well to computed data of the optimal networks.

Table 5. Channel Characteristics at the Outlet of the Optimal Channel Network at Goodwin Creek

	$p_m = 0.5$	$p_m = 0.1$	$p_m = 0.01$	$p_d = 0.5$
<i>Topographic Condition $z = -0.5$ (Constrained Analysis)</i>				
Q , m ³ s ⁻¹	1.235	2.523	4.509	15.950
S , m m ⁻¹	0.00203	0.00203	0.00203	0.00203
H , m	0.35	0.48	0.61	1.05
W , m	8.38	11.39	14.62	25.17
v , m s ⁻¹	0.42	0.46	0.50	0.60
ff	0.292	0.327	0.358	0.426
C_V , m ³ m ⁻³	0.00148	0.00206	0.0027	0.003
P_a , W m ⁻²	2.72	4.09	5.70	11.71
τ_0 , Pa	6.46	8.81	11.34	19.44
<i>Topographic Condition $z = -0.622$ (Unconstrained Analysis)</i>				
Q , m ³ s ⁻¹	1.235	2.523	4.509	15.950
S , m m ⁻¹	0.00156	0.00156	0.00156	0.00156
H , m	0.35	0.48	0.61	1.05
W , m	8.87	12.05	15.47	26.64
v , m s ⁻¹	0.40	0.44	0.48	0.57
ff	0.253	0.282	0.310	0.368
C_V , m ³ m ⁻³	0.00148	0.00206	0.0027	0.003
P_a , W m ⁻²	1.98	2.98	4.16	8.54
τ_0 , Pa	4.99	6.80	8.76	15.00

5. Distribution of P_a in Goodwin Creek

Owing to the dynamic nature of natural river systems, a river network will not satisfy local optimality at a given time and space. However, we theorize that river networks tend to adjust their average properties according to the local optimality hypothesis, toward constant P_a . Applying this theory to natural river networks can help us identify river reaches that deviate most from the local optimality condition as reaches where this adjustment should take place and therefore as potentially unstable river sections.

In the framework of our energy expenditure analysis, the power law expressions of the variation in channel characteristics in a river network in (3a)–(3e) describe only average behavior. Variability around these expressions will exist in a given network. As a result, the energy dissipation rate P_a will vary spatially throughout the network. For instance, *Rodríguez-Iturbe et al.* [1992b] show that under specific conditions, the variance of P_a scales with drainage area as $\text{Var}[P_a] \propto A^{0.5}$. In this section we analyze the variability of P_a as a result of variability in slope scaling in Goodwin Creek.

We investigated the distribution of energy expenditure per unit channel area in the actual topography of Goodwin Creek by superposing the channel properties of the developed optimal network (with optimal downstream hydraulic geometry exponents b , f , and constants a_p , c_p) onto the DEM-extracted river network at Goodwin Creek with observed channel slopes S in every reach. By doing so, we get an idea of the variability of P_a in the Goodwin Creek network compared with the optimal network in its place. The dissipation rate P_a was computed for every point in the river network using (2) and (3a)–(3d):

$$P_a = g\rho_w S \frac{\psi_p A^{\theta(p)} + (G-1)k_p \psi_p^{j+1} A^{(j+1)\theta(p)}}{a_p \psi_p^b A^{b\theta(p)} + 2c_p \psi_p^f A^{f\theta(p)}} \quad (9)$$

where S is the observed channel slope at a point in the network (in reality, average channel slopes were computed for each of the 17 individual reaches of the network).

Figure 8 shows the histograms of the distribution of P_a

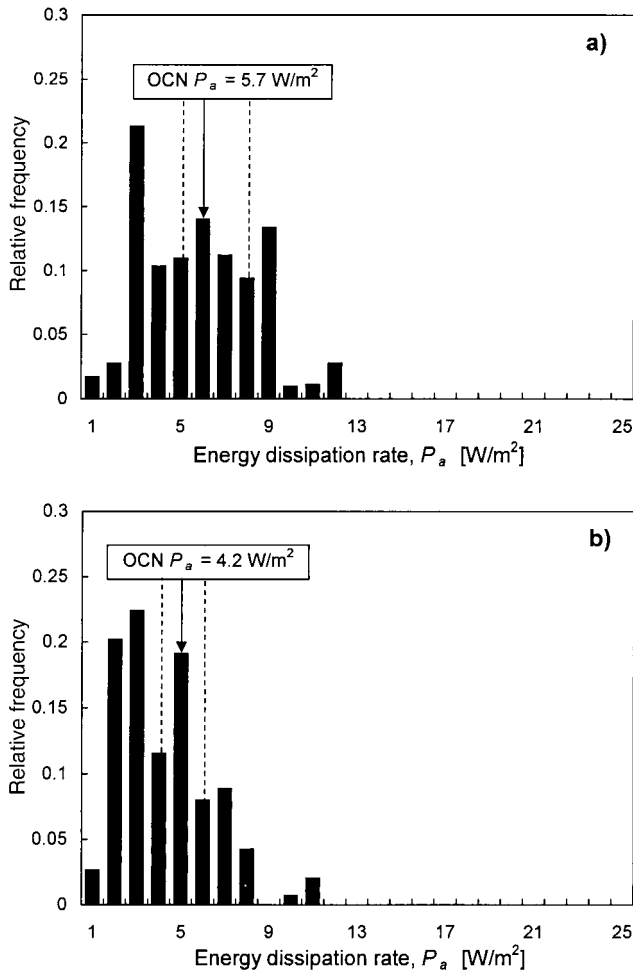


Figure 8. Histograms of the distribution of P_a in Goodwin Creek for the maximum monthly streamflow condition with $p_m = 0.01$ and topographic condition (a) $z = -0.5$ and (b) $z = -0.622$. Optimal (OCN) P_a is depicted with bars representing $\pm 30\%$ change in channel width from optimal.

throughout the Goodwin Creek network using optimal channel geometry parameters for both topographic conditions and maximum monthly discharge. The computed values of P_a are distributed around the constant value representing the optimal network. The constant OCN value was $P_a = 5.7$ W m⁻² ($z = -0.5$) and $P_a = 4.2$ W m⁻² ($z = -0.622$). The variance of P_a was 6.41 (W m⁻²)² ($z = -0.5$) and 4.42 (W m⁻²)² ($z = -0.622$). The reason for the variability in P_a is that the channel reach slopes are different from the slope-scaling prediction of the optimal network. In Figure 8 we also show how variability in channel flow width would influence the distribution of P_a . The dashed lines represent the range of P_a that would correspond to an average 30% decrease or increase in channel flow width from the optimal value throughout the network.

Figure 9 shows similar results for the channel-forming maximum daily streamflow condition. In this case, the distribution of computed energy dissipation rates P_a is wider around the predicted constant value of the optimal network because of the higher flow magnitude. The constant OCN value was $P_a = 11.6$ W m⁻² ($z = -0.5$) and $P_a = 8.5$ W m⁻² ($z = -0.622$). The variance of P_a was 27.1 (W m⁻²)²

($z = -0.5$) and 18.71 (W m⁻²)² ($z = -0.622$). In both cases it is clear that the unconstrained topographic condition $z = -0.622$ provides lower energy expenditure rates and less variability in energy expenditure throughout the network.

It seems indisputable that if the local optimality hypothesis holds, then river reaches that exhibit the largest deviations of P_a from the constant optimal value would theoretically need most channel adjustment to change toward the optimal state. These network reaches may be considered as potentially the most unstable. We therefore explored the spatial distribution of P_a in individual Goodwin Creek reaches. Figure 10 shows the average computed rates of P_a for each of the 17 reaches identified at Goodwin Creek. It is clear from this figure that channel reaches 8, 15, and 4 exhibit higher average dissipation rates than the remainder of the network, while reaches 11, 13, 6, and 17 exhibit average dissipation rates lower than the remainder of the network. The question then remains, whether the average channel properties of these reaches differ from those of the optimal network in the direction of constant P_a , or not. For selected reaches at Goodwin Creek, we attempt to explore this question in the following discussion.

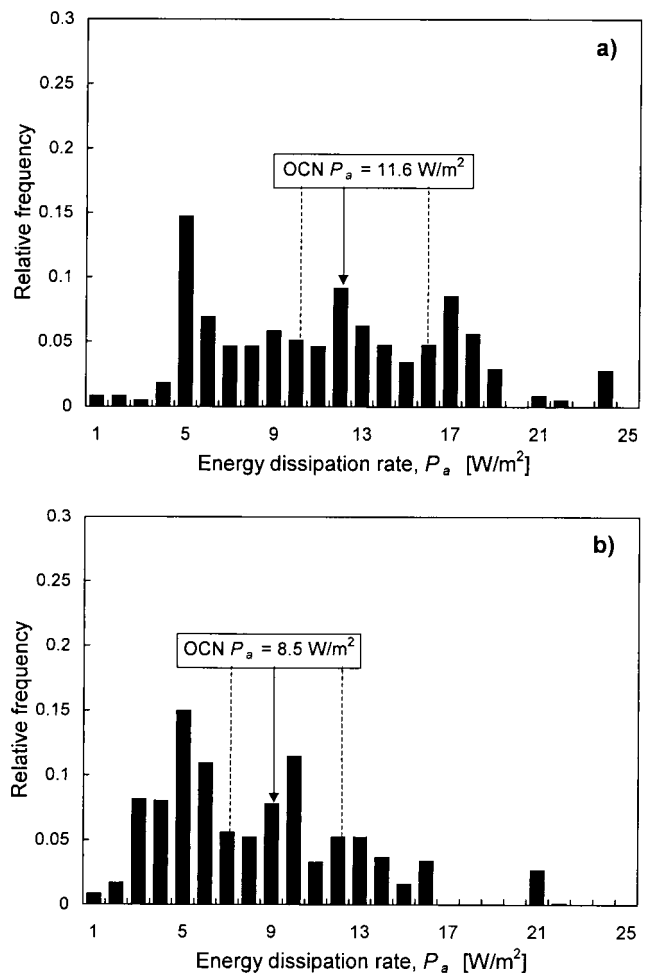


Figure 9. Histograms of the distribution of P_a in Goodwin Creek for the maximum daily streamflow condition with $p_d = 0.5$ and topographic condition (a) $z = -0.5$ and (b) $z = -0.622$. Optimal (OCN) P_a is depicted with bars representing $\pm 30\%$ change in channel width from optimal.

6. Discussion

Based on the hypothesis of local optimality in the preceding sections, optimal channel characteristics were found for Goodwin Creek that assure constant P_a throughout the network. When P_a was computed with these optimal channel characteristics, but with the true channel bed slope in every reach (rather than $S = s A^\varepsilon$), the resulting P_a was no longer constant. The essential argument in this discussion is that if a river network is continuously adjusting to reach equilibrium conditions according to the local optimal energy expenditure hypothesis, then channel reaches with higher than optimal P_a will adjust their properties in order to decrease the rate of energy dissipation, and conversely for sections with lower than optimal P_a . Therefore average channel properties of Goodwin Creek reaches 8, 15, 4, as well as 11, 13, 6, and 17 should differ from the OCN predicted values for those reaches in the direction that would tend to produce constant P_a , or otherwise be unstable. This thesis was explored in Figure 11.

The horizontal axis in Figure 11 shows the difference between average P_a computed with actual reach slopes and average P_a optimal for each reach, $\Delta P_a = P_{a,comp} - P_{a,opt}$. Assuming that the variation of channel flow depth exactly follows the downstream hydraulic geometry relation $H_p = c_p Q_p^f$ (with c_p and f estimated from data), does the channel flow width at individual reaches vary from the predicted optimal value in the direction that would decrease $|\Delta P_a|$ as required by the local optimality hypothesis? Since we did not have measurements of channel flow width (corresponding to each discharge condition studied), we explored this question using the surveyed channel top widths. The vertical axis in Figure 11 shows the difference between the average channel top width W_t and the average predicted optimal value for each reach, $\Delta W = W_t - W_{opt}$. Upstream reaches of the Goodwin Creek river network 1, 2, 3, 6, 9, 12, 14 and 16 draining less than 2 km² were excluded because their surveyed channel top widths did not relate to the actual flow widths. In general, changes in channel flow width and energy dissipation rate P_a from the optimal state are inversely related:

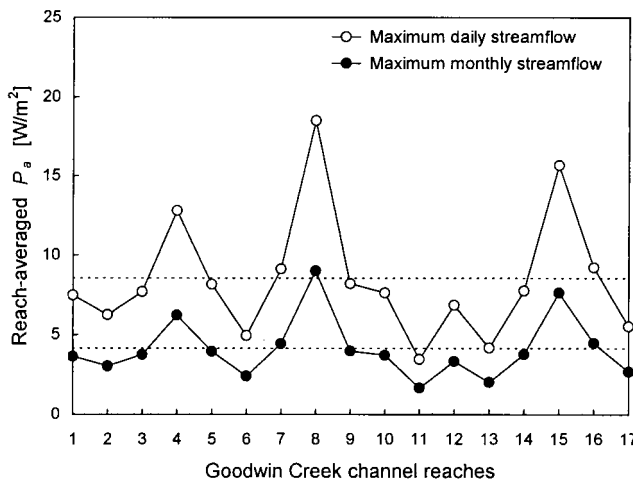


Figure 10. Average energy dissipation rate P_a for each channel reach at Goodwin Creek for maximum monthly and daily discharge conditions with $p_m = 0.01$ and $p_d = 0.5$. Dashed lines are constant OCN P_a for those conditions.

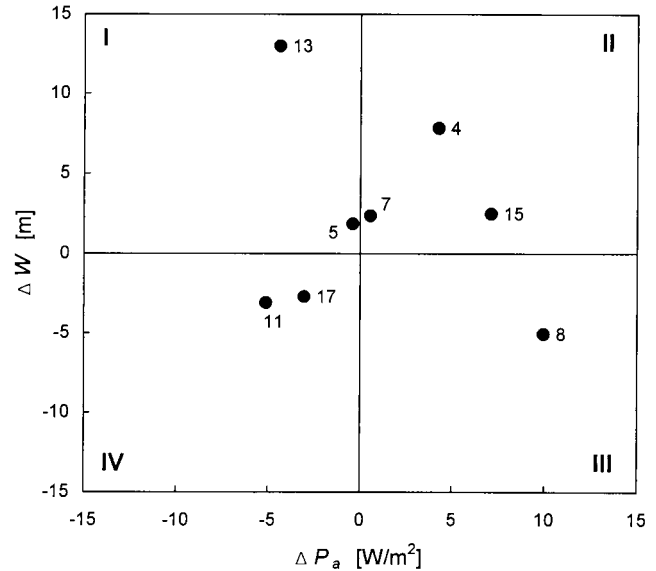


Figure 11. Analysis of the deviations of channel width from the optimal channel network conditions. In regions II and IV, changes are toward constant P_a .

$$(P_{a,opt} + \Delta P_a) = \gamma_m \frac{S Q}{(W_{opt} + \Delta W) + 2H} = \text{const} \quad (10)$$

So in order to attain a constant energy dissipation rate, an increase in channel width ($\Delta W > 0$) would bring about a decrease in the energy dissipation rate ($\Delta P_a < 0$) from the optimal conditions, and vice versa. Based on this, we can conclude that for regions in Figure 11 where $\Delta P_a > 0$ (regions II and III) ΔP_a would decrease if $\Delta W > 0$. This means that reaches that plot in region II have channel width differing from the optimal predicted value in the direction of constant P_a . The same holds true for region IV. This also means that reaches that plot in regions I and III do not have channel width differing from the optimal predicted value in the direction of constant P_a and are potentially unstable. For an exactly optimal river network according to the local optimality hypothesis, the reaches would plot in the center of the graph. The preceding discussion assumes that channel top width is proportional to channel flow width throughout the downstream sections of the network with the same proportionality constant. For the maximum daily streamflow condition (channel-forming flow) studied here, we believe that to be a reasonably good assumption.

Most notable in Figure 11 is that Goodwin Creek reaches 8 and 13 plot in regions I and III and, according to the discussion, can be considered unstable relative to the remainder of the network. We therefore explored the properties and behavior of these channel reaches. *Grissinger and Murphey* [1986] describe the downstream sections of Goodwin Creek (reaches 13, 15, and 17) to be deeply incised, greatly enlarged in places, and highly variable in form with complex channel adjustment. They analyzed the volume changes in these reaches due to erosion and filling for the period from November 1977 to July 1984, based on over 30 channel cross-section surveys. The main conclusion from their analysis is that channel widening due to bank erosion dominated long-term adjustment (with large spatial variability), together with overall channel bed aggradation. Over 60% of total bed filling and 70% of bank erosion occurred in large bend reaches, with significant seasonal variability.

ity [Grissinger and Murphey, 1989]. In the context of our study, we determined that reach 13 experienced bank erosion in the studied period with an average annual volume of 4.28 m³ per meter of channel. Average annual bed aggradation was about 1.25 m³ m⁻¹ during that period. This resulted in considerable channel widening and a decrease in channel bed slope, which is precisely why reach 13 plots in region I in Figure 11. In recent years however, reach 13 has experienced some incision, channel banks had to be stabilized (R. L. Bingner, personal communication, 1997), and knickpoint migration was observed [Blackmarr, 1995]. It has been argued that some of the observed channel change may be attributed to the construction of the flume at gaging station 2 [Grissinger and Murphey, 1986, 1989]. The downstream reaches 15 and 17 on the main stem have also experienced significant channel widening due to bank erosion as well as channel bed aggradation. We estimated average annual bank erosion at 8.16 m³ m⁻¹ in reach 15 and 2.7 m³ m⁻¹ in reach 17, and average annual bed aggradation at 2.39 m³ m⁻¹ in reach 15 and 2.74 m³ m⁻¹ in reach 17 (from data of Grissinger and Murphey [1986]). Goodwin Creek reach 8 has been reported to be an active reach not affected by past channelization works. Unstable banks and channel widening have also been observed in this section in recent years (R. L. Bingner, personal communication, 1997), which would move the reach into region II of Figure 11 (provided channel bed slope changes would be insignificant).

Observations indicate that the downstream sections of Goodwin Creek are undergoing major channel change. However, caution should be exercised in the interpretation of the data, since major bank failures at Goodwin Creek are lithologically controlled (they occur mostly in reaches incised in late Holocene deposits as a result of tension crack development), and are not significantly related to runoff. Similarly, channel bed aggradation seems to be related to sediment availability from upstream, which is seasonally variable and dependent on agricultural practices in the watershed [Grissinger and Murphey, 1989]. In general, some sections of Goodwin Creek are incised into older valley deposits, which influence their adjustment [Blackmarr, 1995]. These are all controlling factors that are not included in our analysis but potentially limit the amount and direction of channel change. They result in the variability in channel characteristics observed in nature.

7. Conclusions

This paper has explored the theory that river networks naturally evolve into structures that are most efficient in the transport of their imposed water and sediment loads. The practical application of the local optimal energy expenditure hypothesis of a constant energy dissipation rate per unit channel area P_a to Goodwin Creek showed the potential of the theory to define the spatial distribution of energy expenditure throughout a river network. Developed optimal channel characteristics were superposed onto the DEM-extracted Goodwin Creek network, and the spatial distribution of the energy dissipation rate P_a was analyzed. Channel reaches with average energy dissipation rates different from the predicted constant value of the optimal network were identified. We argued that these reaches are potentially unstable relative to the remainder of the network and that their mean behavior represented by downstream hydraulic geometry variation should change in the direction that achieves constant P_a (provided they are free to adjust).

Statements were made about the adjustment towards an

equable distribution of P_a at Goodwin Creek through differences between the observed and optimal widths of the river network. On the basis of conditions of local optimality, Goodwin Creek channel reaches 8 and 13 were identified as being unstable relative to the remainder of the network and potentially most prone to future channel adjustment. The validity of this statement was explored on observations of recent channel adjustment at Goodwin Creek. Both reaches were found to be active, with considerable channel widening occurring. Generally, bed aggradation accompanied bank erosion, although net erosion predominated in the downstream sections of the network.

The purpose of this energy expenditure analysis was to show that the hypothesis of local optimality can be a useful tool for studying long-term average channel properties and the relative stability and potential channel adjustment of river networks. The results for Goodwin Creek should be viewed in this perspective.

Acknowledgments. The authors would like to thank the reviewers Rafael L. Bras, Alan D. Howard, Riccardo Rigon, and Brent M. Troutman for their insightful comments to an earlier draft of this paper. We also acknowledge Jane Thurman from the USDA-ARS Hydrologic Data Center, and Carlos Alonso and William Blackmarr from the USDA-ARS National Sedimentation Laboratory for providing the data used in this study.

References

- Bathurst, J. C., Flow resistance through the channel network, in *Channel Network Hydrology*, edited by K. Beven and M. J. Kirkby, pp. 69–98, John Wiley, New York, 1993.
- Blackmarr, W. A. (Ed.), Documentation of hydrologic, geomorphic, and sediment transport measurements on the Goodwin Creek experimental watershed, northern Mississippi, for the period 1982–1993, preliminary release, *Res. Rep. 3*, Natl. Sediment. Lab., Agric. Res. Serv., U.S. Dep. of Agric., Oxford, Miss., 1995.
- Bowie, A. J., and O. W. Sansom, Innovative techniques for collecting hydrologic data, in *Proceedings of the 4th Federal Interagency Sedimentation Conference*, pp. 1/59–1/69, U.S. Gov. Print. Off., Washington, D. C., 1986.
- Bras, R. L., *Hydrology: An Introduction to Hydrologic Science*, pp. 571–572, Addison-Wesley, Reading, Mass., 1990.
- Grissinger, E. H., and J. B. Murphey, Bank and bed adjustments in a Yazoo bluffline tributary, in *Third International Symposium on River Sedimentation*, pp. 1003–1012, Univ. of Miss., University, 1986.
- Grissinger, E. H., and J. B. Murphey, Bank stability of Goodwin Creek channel, northern Mississippi, USA, in *Fourth International Symposium on River Sedimentation*, pp. 59–66, China Ocean Press, Beijing, 1989.
- Gupta, V. K., and D. R. Dawdy, Physical interpretations of regional variations in the scaling exponents of flood quantiles, *Hydrol. Processes*, 9, 347–361, 1995.
- Gupta, V. K., O. J. Mesa, and D. R. Dawdy, Multiscaling theory of flood peaks: Regional quantile analysis, *Water Resour. Res.*, 30(12), 3405–3421, 1994.
- Howard, A. D., Theoretical model of optimal drainage networks, *Water Resour. Res.*, 26(9), 2107–2117, 1990.
- Ijjász-Vásquez, E. J., and R. L. Bras, Scaling regimes of local slope versus contributing area in digital elevation models, *Geomorphology*, 12, 299–311, 1995.
- Julien, P. Y., and J. Wargadalam, Alluvial channel geometry: Theory and applications, *J. Hydraul. Eng.*, 121(4), 312–325, 1995.
- Knighton, D., *Fluvial Forms and Processes*, 218 pp., Edward Arnold, London, 1984.
- Kuhnle, R. A., Fractional transport rates of bed load on Goodwin Creek, in *Dynamics of Gravel-Bed Rivers*, edited by P. Billi et al., pp. 141–155, John Wiley, New York, 1992.
- Kuhnle, R. A., Variations in Bed Material Size on Goodwin Creek, in *Proceedings of the 6th Federal Interagency Sedimentation Conference*, pp. II/68–II/74, U. S. Gov. Print. Off., Washington, D. C., 1996.

- Kuhnle, R. A., J. C. Willis, and A. J. Bowie, Total sediment load calculations for Goodwin Creek, in *International Symposium on Sediment Transport Modelling*, edited by S. S. Y. Wang, pp. 700–705, Am. Soc. of Civ. Eng., New York, 1989.
- Kuhnle, R. A., R. L. Bingner, G. R. Foster, and E. H. Grissinger, Effect of land use on sediment transport in Goodwin Creek, *Water Resour. Res.*, 32(10), 3189–3196, 1996.
- Langbein, W. B., Geometry of river channels, *J. Hydraul. Div. Am. Soc. Civ. Eng.*, 90(HY2), 301–312, 1964.
- Langbein, W. B., and L. B. Leopold, Quasi-equilibrium states in channel morphology, *Am. J. Sci.*, 262, 782–794, 1964.
- Leopold, L. B., and W. B. Langbein, The concept of entropy in landscape evolution, *U. S. Geol. Surv. Prof. Pap.*, 500-A, 20 pp., 1962.
- Leopold, L. B., and T. Maddock, The hydraulic geometry of stream channels and some physiographic implications, *U. S. Geol. Surv. Prof. Pap.*, 252, 57 pp., 1953.
- Molnár, P., Energy dissipation in a river network, M.S. thesis, 158 pp., Colo. State Univ., Fort Collins, 1996.
- Molnár, P., and J. A. Ramírez, Energy dissipation theories and optimal channel characteristics of river networks, *Water Resour. Res.*, this issue.
- Park, C. C., World-wide variations in hydraulic geometry exponents of stream channels: An analysis and some observations, *J. Hydrol.*, 33, 133–146, 1977.
- Petts, G., and I. Foster, Channel morphology, in *Rivers and Landscape*, pp. 140–174, Edward Arnold, London, 1985.
- Rigon, R., A. Rinaldo, I. Rodríguez-Iturbe, R. L. Bras, and E. J. Ijász-Vásquez, Optimal channel networks: A framework for the study of river basin morphology, *Water Resour. Res.*, 29(6), 1635–1646, 1993.
- Rinaldo, A., I. Rodríguez-Iturbe, R. Rigon, R. L. Bras, E. J. Ijász-Vásquez, and A. Marani, Minimum energy and fractal structures of drainage networks, *Water Resour. Res.*, 28(9), 2183–2195, 1992.
- Rodríguez-Iturbe, I., and A. Rinaldo, *Fractal River Basins: Chance and Self-Organization*, 547 pp., Cambridge Univ. Press, New York, 1997.
- Rodríguez-Iturbe, I., A. Rinaldo, R. Rigon, R. L. Bras, A. Marani, and E. J. Ijász-Vásquez, Energy dissipation, runoff production, and the three-dimensional structure of river basins, *Water Resour. Res.*, 28(4), 1095–1103, 1992a.
- Rodríguez-Iturbe, I., E. J. Ijász-Vásquez, R. L. Bras, and D. G. Tarboton, Power law distributions of discharge mass and energy in river basins, *Water Resour. Res.*, 28(4), 1089–1093, 1992b.
- Stedinger, J. R., R. M. Vogel, and E. Foufoula-Georgiou, Frequency analysis of extreme events, in *Handbook of Hydrology*, edited by D. R. Maidment, pp. 18.22–18.29, McGraw-Hill, New York, 1992.
- Tarboton, D. G., A new method for the determination of flow directions and upslope areas in grid digital elevation models, *Water Resour. Res.*, 33(2), 309–319, 1997.
- Tarboton, D. G., R. L. Bras, and I. Rodríguez-Iturbe, Scaling and elevation in river networks, *Water Resour. Res.*, 25(9), 2037–2051, 1989.
- Troutman, B. M., Inference for a channel network model and implications for flood scaling, in *Reduction and Predictability of Natural Disasters*, edited by J. B. Rundle, D. L. Turcotte and W. Klein, pp. 97–116, Addison-Wesley, Reading, Mass., 1996.
- Willis, J. C., R. W. Darden, and A. J. Bowie, Sediment transport in Goodwin Creek, in *Proceedings of the 4th Federal Interagency Sedimentation Conference*, pp. 4/30–4/39, U. S. Gov. Print. Off., Washington, D. C., 1986.
- Yang, C. T., Potential energy and stream morphology, *Water Resour. Res.*, 7(2), 311–322, 1971.
- Yang, C. T., and C. C. S. Song, Theory of minimum rate of energy dissipation, *J. Hydraul. Div. Am. Soc. Civ. Eng.*, 105(HY7), 769–784, 1979.
- Yang, C. T., and C. C. S. Song, Theory of minimum energy and energy dissipation rate, in *Encyclopedia of Fluid Mechanics*, edited by N. D. Chermisinoff, pp. 353–399, Gulf, Houston, Tex., 1986.

P. Molnár and J. A. Ramírez, Department of Civil Engineering, Colorado State University, Fort Collins, CO 80523. (e-mail: molnarp@lamar.colostate.edu; ramirez@tayrona.engr.colostate.edu)

(Received March 25, 1997; revised February 6, 1998; accepted March 20, 1998.)

